International Journal of
Molecular Sciences

MDPI

Article

Electrochemically Reduced Graphene Oxide Covalently Bound Sensor for Paracetamol Voltammetric Determination

Amaya Paz de la vega [1], Fabiana Liendo [1], Bryan Pichún [1,2], Johisner Penagos [1], Rodrigo Segura [1,*] and María Jesús Aguirre [1,2,*]

[1] Department of Chemistry of Materials, Faculty of Chemistry and Biology, Universidad de Santiago de Chile (USACH), Santiago 9170022, Chile; amaya.pazdelavega@usach.cl (A.P.d.l.v.)
[2] Millennium Institute on Green Ammonia as Energy Vector—MIGA (ICN2021_023), Santiago 7820436, Chile
* Correspondence: rodrigo.segura@usach.cl (R.S.); maria.aguirre@usach.cl (M.J.A.)

Abstract: Designing a highly sensitive and efficient functionalized electrode for precise drug analysis remains a significant challenge. In this work, an electrochemical sensor based on a glassy carbon electrode (GCE) modified with phenyl diazonium salts (ph) and electrochemically reduced graphene oxide (ERGO), labeled GCE/ph/ERGO, was developed for the detection of paracetamol (PAR) in pharmaceutical matrices using square wave voltammetry (SWV). The modified electrode was characterized by scanning electron microscopy (SEM), electrochemical impedance spectroscopy (EIS), and cyclic voltammetry (CV). Compared to the bare GCE, the GCE/ph/ERGO sensor demonstrated significantly improved conductivity and anodic current peak for PAR over two orders of magnitude higher, indicating a substantial enhancement in electrochemical performance. Under optimized conditions, the developed sensor exhibited a low detection limit of 18.2 nM and a quantification limit of 60.6 nM. Precision studies yielded relative standard deviations (RSDs) below 8%. The sensor demonstrated excellent selectivity in the presence of common pharmaceutical excipients and high accuracy in the analysis of generic pharmaceutical formulations, with results comparable to those obtained by the HPLC technique. These findings confirm the sensor's reliability, stability, robustness, and suitability for routine analysis of PAR in pharmaceutical samples.

Keywords: electrochemical grafting; 4-nitroaniline; reduced graphene oxide; paracetamol; square wave voltammetry; pharmaceutical tablets

Academic Editor: Christian Julien

Received: 21 March 2025
Revised: 24 April 2025
Accepted: 28 April 2025
Published: 30 April 2025

Citation: Paz de la vega, A.; Liendo, F.; Pichún, B.; Penagos, J.; Segura, R.; Aguirre, M.J. Electrochemically Reduced Graphene Oxide Covalently Bound Sensor for Paracetamol Voltammetric Determination. *Int. J. Mol. Sci.* **2025**, *26*, 4267. https://doi.org/10.3390/ijms26094267

1. Introduction

Paracetamol (acetaminophen) is an over-the-counter medication that has an analgesic and antipyretic effect, used for the treatment of fever and mild to moderate pain [1]. It is well tolerated and has a minimal risk of gastrointestinal side effects. When misused or overdosed, paracetamol is also capable of inducing serious hepatic damage, which can lead to life-threatening liver necrosis [2]. Chronic use by itself is typically harmless, but when combined with other acetaminophen-containing medications, it presents a substantial risk of toxicity [3]. In fact, acetaminophen toxicity is the second leading cause of liver transplants worldwide [4,5].

These risks highlight the need for an effective quality control system in the pharmaceutical industry to ensure drug safety [6–8]. These quality control procedures are conducted to guarantee the identity, purity, and concentration of a particular pharmaceutical product, generating the desired pharmacological effect without causing adverse effects or overdose,

to improve the safety and efficacy of these products, and to help keep the public healthy and safe.

The analysis of pharmaceutical compounds in aqueous matrices or pharmaceutical preparations is predominantly performed using chromatographic techniques, such as liquid chromatography (HPLC) coupled with mass spectrometers (MS) [9]. Although these techniques offer low detection limits and high sensitivity, their high acquisition and maintenance costs, along with the impossibility of using this technique "in situ", have promoted the development of faster and more accessible techniques. Voltammetric techniques provide reliable results in terms of reproducibility and repeatability, low detection limits, easy implementation, and low-cost, low-maintenance instrumentation. Moreover, they are well-suited for use in portable systems [10–14]. However, most solid electrodes used for electroanalysis of organic molecules (e.g., glassy carbon, screen-printed, boron-doped diamond, and gold electrodes) have limitations, including surface fouling, small surface area, signal drift or sensitivity loss, and limited selectivity [15]. To overcome some of these disadvantages, chemically modified electrodes (CMEs) are being explored for sensitivity, selectivity, and stability improvements, which are based on the generation of a film of a modifying agent on the surface of an electrode, improving the sensitivity and selectivity of the measurement [16–19]. Various modifying agents have been used, ranging from metallic deposits to organic materials. They can be prepared by different methods, one of which is physisorption or "drop-coating", which consists of applying a thin coating of a chemical compound, such as a carbon nanomaterial, by depositing consecutive drops of a suspension on the electrode surface and allowing the solvent to evaporate. Another surface modification technique is "electrografting", an electrochemical reaction where a molecule, a diazonium salt, for example, is reduced or oxidized on the working electrode [20–23], granting great sensor stability resulting from the covalent bond between the modifier and the electrode surface. Electrochemically reduced graphene oxide (ERGO), a two-dimensional carbon nanomaterial that allows for easy access and synthesis, low cost, and simple functionalization [24–26], is among the nanomaterials used to modify an electrode. ERGO has been the subject of investigation in many technological fields over the past decades, including chemical sensors, biosensors/immunosensors, and nanocomposites. Electrochemical surfaces modified with ERGO have been extensively studied due to ERGO's high surface area, excellent biocompatibility, and outstanding electrocatalytic and antifouling properties, making it effective for the detection of various molecules and biomolecules [19,27,28]. ERGO can be integrated onto electrode surfaces via several strategies, including physical adsorption or covalent attachment of functional groups [29]. Among these, diazonium chemistry offers a particularly robust approach for forming stable graphene-based films. Diazonium intermediates exhibit very low reduction potentials, enabling stable functionalization across a wide range of substrates without risk of oxidation. They are also water-compatible and can be generated from various aromatic amines [22,30,31]. These diazonium-derived organic layers exhibit excellent electron transfer properties, facilitating efficient charge transport between the electrode and the analyte. Reactions involving diazonium salts have been widely used to covalently functionalize metals, semiconductors, and carbon-based materials such as carbon nanotubes and graphene nanosheets [32].

Anchoring ERGO onto electrode surfaces via diazonium salt chemistry further enhances electrochemical sensor performance. ERGO improves electron transfer and conductivity, while its porous structure offers more active sites, thereby increasing sensitivity and current response. The strong covalent bonding provided by diazonium chemistry contributes to long-term stability and allows for surface tailoring to improve selectivity or antifouling behavior. Moreover, by carefully controlling the concentration of diazo-

nium salts and the grafting conditions, multilayer formation can be avoided, preserving ERGO's inherent conductivity and electroactivity. This composite strategy leads to reproducible, stable, and sensitive electrochemical platforms suitable for detecting organic analytes [33–35].

While many studies have focused on the covalent attachment of carboxyl-functionalized graphene using carbodiimide coupling chemistry [36,37], the use of diazonium chemistry to covalently anchor ERGO remains comparatively unexplored. Furthermore, although paracetamol detection has been widely studied using both carbon and graphene-based electrodes, the synergistic integration of phenyl diazonium salts with ERGO to construct high-performance sensing interfaces has received limited attention.

In this work, a glassy carbon electrode modified with electrochemically reduced graphene oxide via phenyl diazonium salt chemistry (GCE/ph/ERGO) was developed. The combination of ERGO and diazonium modification enhances sensor surface stability, conductivity, and sensitivity toward phenolic compounds such as paracetamol in pharmaceutical formulations, outperforming electrodes modified with physiadsorbed ERGO alone.

2. Results and Discussion

To obtain a highly conductive and sensitive sensing interface, we aimed to enhance the properties of ERGO through a controlled modification strategy. By introducing a conductive molecular anchor, we promoted ERGO attachment, avoiding agglomeration and preserving its electrochemical activity, improving the sensor's performance in PAR detection.

2.1. Electrografting Process and Surface Fabrication

To ensure the formation of a controlled and thin aryl layer on the GCE surface, the electrografting conditions were carefully optimized: (i) a low concentration (1 mM) of the aromatic amine was used to limit aryl radicals generation and minimize multilayer formation; (ii) electrochemical grafting was performed via cyclic voltammetry using only two potential cycles within a narrow window, sufficient to initiate diazonium reduction without excessive radical accumulation or over-grafting; (iii) 4-nitroaniline was selected as the aromatic amine precursor due to the electron-withdrawing nitro group, which introduces electronic repulsion and steric hindrance, thereby reducing the likelihood of secondary aryl–aryl radical coupling and favoring monolayer formation [38,39].

In the first stage, p-nitrophenyl diazonium cations are generated in acid media using pNA and $NaNO_2$ as precursors in the electrochemical cell. In the second stage, the covalent modification is carried out using electrografting or electrochemical reduction of the GCE surface with the p-nitrophenyl diazonium cations by CV. The molecule is reduced to a radical through the release of molecular nitrogen, and this aryl radical reacts with the nearest nucleophile or material, in this case, the electrode surface. In the third stage, the nitro groups on the surface are electrochemically reduced to amino groups to covalently anchor the nanomaterials to the sensor (see Figure 1A).

Figure 1B(i) shows the voltammogram obtained for the electrochemical reduction of p-nitrophenyl diazonium cations. The phenyl diazonium salt was generated "in situ" in the electrochemical cell. An irreversible reduction peak is observed around 0.01 V in the first cycle, consistent with the evidence reported regarding the formation of the diazonium radical using pNA by electrochemical methods (Equation (1)) [29,40]. This broad reduction peak is not observed in the second cycle, which indicates that the grafting process of the GCE surface with the p-nitrophenyl diazonium cations takes place in the first voltammetric cycle, and this grafted layer inhibits further reduction of nitrophenyl diazonium salts onto the GCE surface [41]. A redox peak at 0.33 V (oxidation) (Equation (3)) and 0.27 V

(reduction) (Equation (2)) is observed in subsequent cycles and can be associated with the oxidation of hydroxyamino groups (Equation (3)) generated by a partial reduction of nitro groups (Equation (2)) present in the solution or the modified layer.

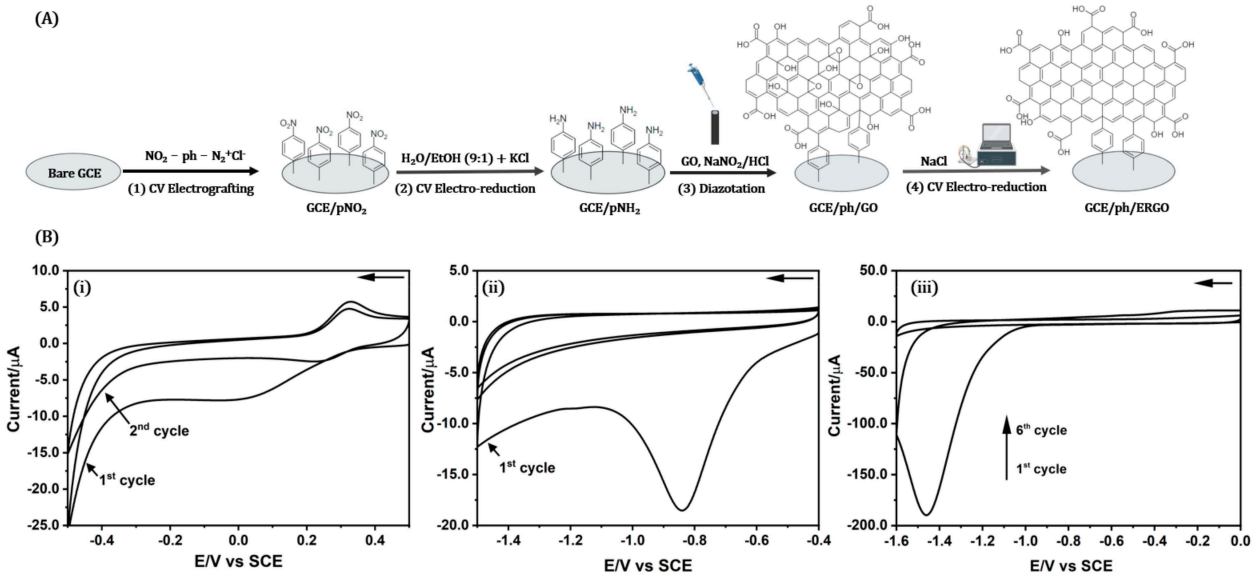

Figure 1. (**A**) Schematic illustration of the electrochemical procedure for GCE/ph/ERGO fabrication. (**B**) Recorded voltammograms for GCE/ph/ERGO fabrication: (**i**) CV of electrochemical reduction of p-nitrophenyl diazonium on the surface of bare GCE in 0.50 M HCl containing 1 mM pNA and 1 mM $NaNO_2$, from 0.50 to −0.50 V, with a scan rate of 100 mV s^{-1}; (**ii**) CV of electrochemical reduction of p-nitrophenyl groups to p-aminophenyl groups present on the surface of GCE/p-NO_2 in 0.10 M KCl in ethanolic solution (9 mL H_2O + 1 mL EtOH), from −0.40 to −1.50 V, with a scan rate of 50 mV s^{-1}; and (**iii**) CV of electrochemical reduction of GCE/ph/GO to GCE/ph/ERGO in 0.25 M NaCl solution, from 0.0 to −1.60 V, with a scan rate of 50 mV s^{-1} (arrow indicates sweep direction).

$$Ar - NO_2 + e^- \rightarrow Ar - NO_2 \cdot \quad (1)$$

$$Ar - NO_2 + 4H^+ + 4e^- \rightarrow Ar - NHOH + H_2O \quad (2)$$

$$Ar - NHOH \leftrightarrow Ar - NO + 2H^+ + 2e^- \quad (3)$$

$$Ar - NHOH + 2H^+ + 2e^- \rightarrow Ar - NH_2 + H_2O \quad (4)$$

The modified p-nitrophenyl groups on the surface of GCE/pNO_2 are electrochemically reduced to p-aminophenyl groups by CV in a protic solution (0.10 M KCl in 90:10 v/v H_2O/EtOH). The voltammogram obtained (Figure 1B(ii)) shows a cathodic peak at −0.84 V, associated with the irreversible electroreduction of p-nitrophenyl to p-aminophenyl in a six-proton, six-electron process (through a mechanism 4 + 2e^-) carried out in the modified layer (Equations (2) and (4)) [42,43].

In this work, we incorporated GO nanomaterials into the modified electrode through the diazotation of the amino groups present in the GCE/p-NH_2 surface and the immediate anchoring of GO through drop-casting of a GO and $NaNO_2$ acid solution, followed by electrochemical reduction of this GO layer.

Our investigation team previously reported [44] the optimal conditions for the irreversible electrochemical reduction of graphene oxide in aqueous solution. The process is conducted using cyclic voltammetry, applying five reduction cycles between 0.00 and −1.60 V. In Figure 1B(iii), a cathodic peak can be seen at −1.46 V, associated with the presence of epoxide, hydroxyl, and carboxylic acid groups in the GO structure. After

the irreversible electroreduction of these oxygenated groups, we obtain electrochemically reduced graphene oxide on the electrode surface (GCE/ph/ERGO).

2.2. Morphological Characterization of the Modified Surface

The surface morphologies were investigated by SEM. Figure 2A shows SEM images of bare GCE. The surface morphology of GCE/p-NH_2 (Figure 2B) shows no significant difference from bare GCE, indicating that the organic film formed does not influence the electrode surface morphology. In comparison, GCE/ph/ERGO (Figure 2C,D) shows modification of the nanomaterial in the form of white "wrinkled" layers on the surface.

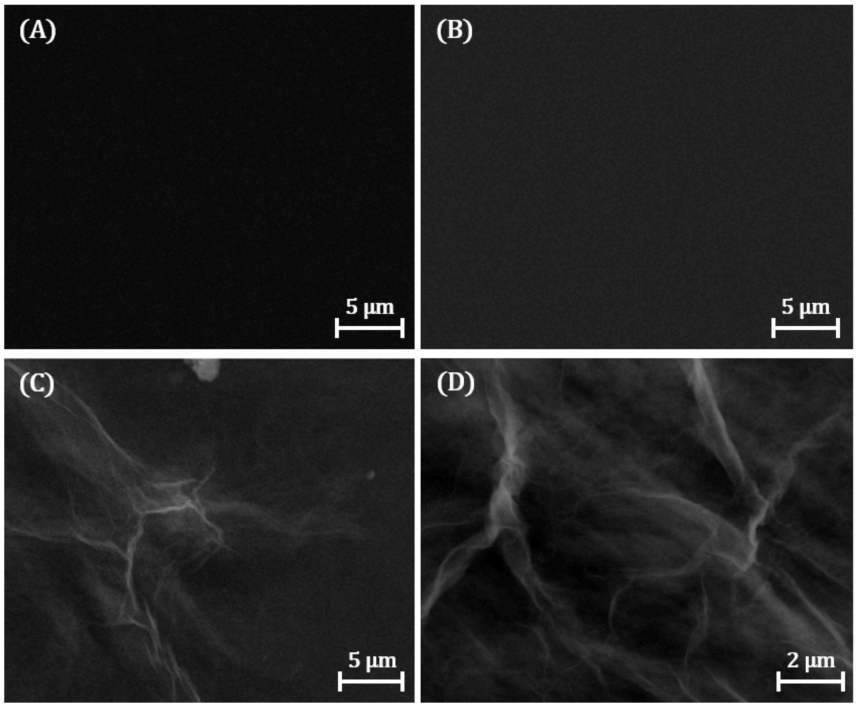

Figure 2. SEM images of (**A**) bare GCE, (**B**) GCE/p-NH_2, and (**C**,**D**) GCE/ph/ERGO sensing interfaces.

2.3. Electrochemical Characterization of Modified Surface

All modified surfaces were characterized using CV and electrochemical impedance spectroscopy (EIS) in a solution containing the redox species ferro and ferricyanide ($Fe(CN)_6^{3-/4-}$). Figure 3A shows pronounced anodic and cathodic peaks for the GCE electrode characteristic of single-electron transfer of the redox couple (ΔE 0.07 V). The diazonium grafted surface (GCE/p-NO_2) reported an increase in charge transfer resistance and suppression of the $Fe(CN)_6^{3-/4-}$ anodic and cathodic peaks, which confirmed successful surface modification consistent with a thin, covalently attached aryl layer. However, after electroreduction of the p-nitrophenyl groups to p-aminophenyl (GCE/p-NH_2), the cathodic and anodic signals of the redox couple are recovered to some extent, with a decrease in current intensity compared to GCE (ΔE 0.10 V), which would indicate the generation of an organic film on the electrode surface that would impede electron transfer to a certain extent [45]. Incorporating GO by drop-casting and then electrochemically reducing it to ERGO (GCE/ph/ERGO) recovers the electronic transfer from the electrode surface, with an increase in the current intensity (ΔE 0.06 V) at levels comparable to the electrochemical response of an electrode modified with only ERGO (GCE/ERGO) (ΔE 0.08 V). This behavior is reflected in the results obtained using the EIS technique.

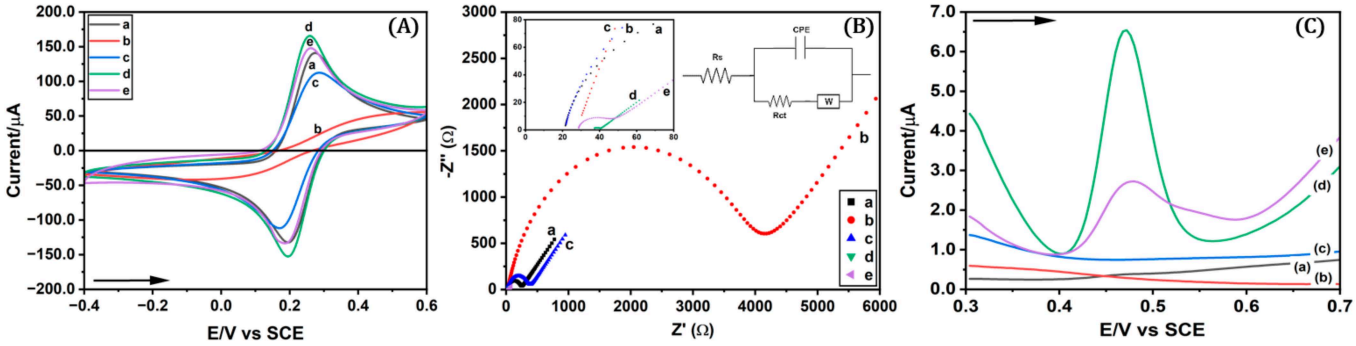

Figure 3. (**A**). Cyclic voltammograms and (**B**) Nyquist plots obtained for characterization in 5 mM $Fe(CN)_6^{3-/4-}$ 0.10 M KCl and 0.10 M PBS pH 7, range −0.40 to 0.60 V, 100 mV s^{-1}, scanning in a frequency range from 0.10 to 100,000 Hz (inset: electrical circuit used to process EIS spectra) (arrow indicates sweep direction). (**C**) Electrochemical performance in the presence of PAR 2 μM in 0.10 mol L^{-1} acetate buffer pH 5 for (a) GCE, (b) GCE/pNO_2, (c) GCE/pNH_2, (d) GCE/ph/ERGO, and (e) GCE/ERGO.

Figure 3B shows the Nyquist diagrams corresponding to GCE and the modified surfaces obtained from the impedance spectrum processed with a Randles equivalent electrical circuit. This model consists of the ionic resistance of the solution (Rs) connected in series to a constant phase element (CPE) that represents the capacitance of the double layer, which in turn is connected in parallel to a Warburg element (W) representing the diffusional resistance and resistance to electron transfer (Rct). The Rct is represented in the Nyquist diagram as the diameter of the semicircle formed and controls the rate of electron transfer at the interface of the redox probe between the solution and the electrode. Once the EIS results have been processed with the equivalent circuit, the Rct values can be obtained. The Rct value for the GCE electrode (Rct 211.27 Ω) increases substantially (Rct 3894 Ω) after modifying the surface with pNA in GCE/p-NO_2. This response may result from the low conductivity of the p-nitrophenyl organic layer, which would hinder the electronic transfer of the redox couple to the electrode surface. After the electro-reduction of the p-nitrophenyl groups to p-aminophenyl, the charge transfer between the couple and the electrode surface becomes more efficient (Rct 338.57 Ω), probably due to the good conductivity of the p-aminophenyl layer. These results coincide with CV studies and are like those found in the bibliography [46–49]. A significant decrease in the Rct (Rct 3.24 Ω) value can be observed after attaching ERGO to the GCE/ph/ERGO modified surface due to the excellent electronic transfer of the nanomaterial, attributed to the partial restoration of the sp^2 carbon network following the electroreduction [50].

2.4. Surface Area of Modified Electrodes

The surface coverage of diazonium salt-modified electrodes GCE/p-NO_2 and GCE/p-NH_2 was estimated using Equation (5), where Γ (mol cm^{-2}) represents the surface coverage, A is the electrode geometric surface area (cm^2), n is the number of electrons involved in the reaction, F is the Faraday constant (C mol^{-1}), and Q is the total amount of charge (C) obtained by integrating the reduction peak recorded using CV. Assuming a four-electron process for the grafting of p-nitrophenyl diazonium cations (Equation (2)) and a six-electron process for the total reduction of p-nitrophenyl to p-aminophenyl groups (Equations (2) and (4)) [41], the surface coverage values calculated from the voltammetric charges (Figure 1A,B) were 1.41×10^{-10} mol cm^{-2} for GCE/p-NO_2 and 1.74×10^{-10} mol cm^{-2} for GCE/p-NH_2. These values are consistent with

previously reported studies for surfaces modified with p-nitrophenyl groups and fall within the expected range for a close-packed monolayer of grafted phenyl groups [31,51–54].

$$\Gamma = \frac{Q}{nFA} \quad (5)$$

The electroactive surface area (ECSA) of GCE, GCE/ph/ERGO, and GCE/ERGO electrodes was estimated using the Randles–Sevcik equation (Equation (6)), where D is the diffusion coefficient of the redox probe (7.6×10^{-6} cm^2 s^{-1}), C the concentration of the redox species (5.0 μmol mL^{-1}), n is the number of electrons transferred (n = 1), ν is the voltammetric scan rate (mV s^{-1}), and A is the electroactive surface area (cm^2) [44,55]. For a diffusion-controlled process, the peak current is linearly dependent on the square root of the scan rate (Figure S1). Based on the slopes obtained from this linear relation, the ECSA was calculated to be 0.10 cm^2 for GCE, 0.13 cm^2 for GCE/ph/ERGO, and 0.14 cm^2 for GCE/ERGO. These results indicate a 30% increase in ECSA for GCE/ph/ERGO and a 40% increase for GCE/ERGO compared to bare GCE, confirming the successful surface modification and enhanced electrochemical activity of the modified electrodes.

$$Ip = 2.69 \times 10^5 \, nACD^{1/2}v^{1/2} \quad (6)$$

2.5. Electrochemical Behavior of PAR at the Modified Electrode

The electrochemical response of the PAR analyte at the GCE and modified surfaces was studied in acetate buffer using square wave voltammetry (Figure 3C). From the voltammogram obtained, the oxidation peak of PAR can be observed at 0.47 V in concordance with the literature [56–58]. According to several studies, PAR exhibits quasi-reversible redox behavior, characterized by a well-defined anodic peak corresponding to the oxidation of the phenolic group to N-acetyl-p-benzoquinone imine (NAPQI) via a two-electron, two-proton process (Scheme 1) [16,59–61].

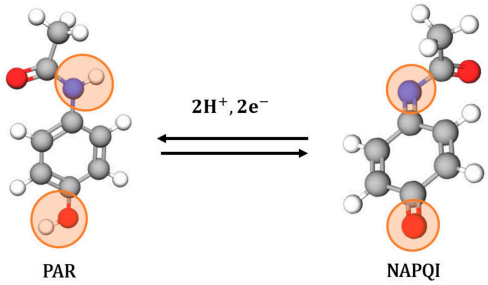

Scheme 1. Electrochemical oxidation mechanism of paracetamol (PAR) to N-acetyl-4-quinoneimine (NAPQI).

Compared with GCE, GCE/p-NH_2, and GCE/ERGO, the GCE/ph/ERGO modified electrode has the highest current response to PAR, which can be attributed to the increased electroactive surface area, high electron mobility, and favorable π–π interactions between paracetamol and the graphene sheets present in the modification. Based on the CV, EIS, and SWV results, the GCE/ph/ERGO electrode showed greater electronic transfer and current response to the analyte compared with non-modified GCE, diazonium-modified surfaces, and the GCE/ERGO electrode.

2.6. Effect of Experimental Variables

2.6.1. Optimization of the Electrografting Process

To optimize the modifier concentration used in the electrografting process to find the best combination to preserve electronic transfer and generate an organic layer, a study of the effect of $NaNO_2$ concentration on the diazotization process was performed by keeping

the pNA concentration at 1 mM and varying the $NaNO_2$ concentration between 1 and 3 mM. Figure S2 shows the electrochemical characterizations of these GCE/p-NH_2 electrodes using CV and EIS in a solution containing the redox species $Fe(CN)_6^{3-/4-}$. GCE and GCE/p-NH_2 with 1 mM pNA and 1 mM $NaNO_2$ (1:1) exhibit the behavior described for the redox couple (Figure 3A). However, as the $NaNO_2$ concentration in the cell increases, it can be observed that the anodic and cathodic peaks of $Fe(CN)_6^{3-/4-}$ progressively decrease their current intensity and move to higher potentials (Figure S2A), increasing the separation between peaks compared to GCE, which is consistent with the modification of the electrode and the generation of an organic layer on the electrode surface that acts as a barrier and prevents the electronic transfer to the electrode surface. The same behavior is observed in the Nyquist plots obtained using EIS (Figure S2B) for the modified surfaces; as the concentration of sodium nitrite increases, the Rct value increases due to the generation of an organic multilayer on the surface. Using a 1:1 concentration in the electrografting process, the best electron transfer results for the modified surface are obtained.

2.6.2. Optimization of Modified GO/$NaNO_2$/HCl Agent

The effect of the volume of the GO modifier aliquot deposited on the surface of the modified electrode was evaluated on the current signal of 2 µM of PAR. For this purpose, the surface was modified with different aliquots of the 0.62 g L^{-1} GO solution, and its effect on the analyte current was studied. As shown in Figure S3, as the volume of the GO modifier aliquot increases, the current signal for PAR increases up to a maximum of 5 µL. At higher modifier volumes, a decrease in the PAR current signal is observed due to a saturation of the electrode surface, which would hinder the charge transfer at the electrode–solution interface.

2.6.3. Optimization of Supporting Electrolyte and pH

As the electrochemical oxidation of PAR is a proton-coupled electron transfer reaction (see Scheme 1), one would expect to observe a dependence on the supporting electrolyte and its pH.

The effect of different supporting electrolytes on the current signal of 2 µM PAR was evaluated using the following buffer systems: acetic acid/acetate (HAc/Ac^-, pH 5), phosphate (PBS, pH 7), Britton–Robinson (pH 6.3), ammonia (pH 8.5), and 0.1 M sulfuric acid (H_2SO_4). According to the literature, PAR exhibits good electrochemical response in HAc/Ac^-, PBS, and Britton–Robinson buffers at pH values below 8 [60,62–64], as it is more stable in slightly acidic to neutral conditions. These pH environments help prevent PAR degradation and improve electrode surface stability. For this work, the best electrochemical response for PAR was obtained using HAc/Ac^- buffer (Figure S4A). Notably, in ammonia buffer (pH 8.5), a significant shift toward more negative potentials and a decrease in current signal were observed. This behavior is attributed to the easier deprotonation of PAR in basic media, resulting in its deprotonated form, which is less adsorptive and potentially less electrochemically active [65]. On the other hand, when using H_2SO_4 as the supporting electrolyte, a significant shift toward more positive potentials was observed, likely due to the extremely acidic environment promoting PAR degradation. The signal may correspond to p-aminophenol, a known acid hydrolysis product of paracetamol, which is electroactive and can be detected by voltammetric techniques within this potential range [66,67].

The effect of pH on the current response of 2 µM PAR was evaluated using the GCE/ph/ERGO sensing interface in 0.10 M HAc/Ac^- buffer over the range 3.50–5.50 (Figure S4B). The maximum current was observed at pH 5. This behavior is likely due to a balance between proton availability and electron transfer efficiency, as the neutral form of PAR—which predominates below pKa of 9.46—is more electroactive at pH 5. At low pH values, excessive protonation of either PAR or the

electrode surface may hinder electron transfer or promote side reactions. Conversely, at high pH values, the deprotonated form of PAR may be less electroactive or adsorptive on the electrode surface (see Figure S5 for reaction). As the pH increases from 3 to 5, the oxidation signal improves, probably due to enhanced deprotonation of the phenolic hydroxyl group, which facilitates a proton-coupled electron transfer (PCET) mechanism [68]. Although paracetamol is expected to remain largely protonated and electrochemically active across the pH range tested, the observed current signal trend suggests a strong influence of the electrode surface properties. As supported by previous studies on molecule–surface interactions, changes in the surface charge can affect local interface behavior through the charge regulation phenomenon [69,70]. Specifically, the analyte and the surface dynamically influence each other's protonation state, potentially shifting the apparent pKa of the analyte. This may explain the enhanced signal at pH 5 and its subsequent decline at pH 5.5, even though bulk protonation remains relatively constant. Further studies will be conducted to determine if there is a surface effect on the displacement of pKa.

2.7. Analytical Performance Evaluation

2.7.1. Linear Range and Limit of Detection

To obtain the linear range and the limit of detection (LOD) and quantification (LOQ), a calibration curve was fabricated with the GCE/ph/ERGO electrode by SWV under optimized conditions of 1 mM pNA and 1 mM $NaNO_2$ in the electrografting process, 5 µL of the GO/$NaNO_2$/HCl agent, and 0.10 M acid/acetate buffer pH 5. Figure 4A,B shows the voltammograms and calibration curve for 0.10–0.80 µM PAR. The LOD and LOQ were calculated using the standard deviation of the intercept, as previously reported [44,55,71–75], and the values obtained were 18.20 and 60.60 nM, respectively. The sensitivity from the slope of calibration plots was 2.46 µA μM^{-1}. The analytical performance of the developed GCE/ph/ERGO sensor for PAR determination compared to other electrochemical surfaces is represented in Table 1. Compared to previously reported sensors for paracetamol detection, our sensor's excellent performance indicates its potential for applications in pharmaceutical quality control. From Table 1, it is easy to deduce that it is one of the best sensors in terms of LOD.

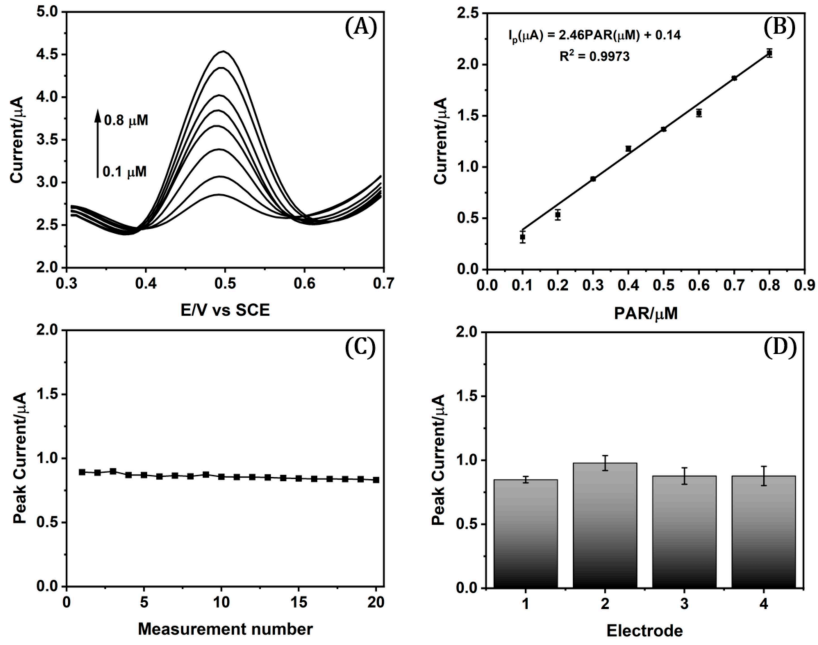

Figure 4. (**A**) SWV voltammograms and (**B**) calibration curve under optimized conditions of PAR. (**C**) Repeatability and (**D**) reproducibility analysis performed with 0.30 µM PAR.

Table 1. Merits of carbon nanomaterial-modified electrodes used in PAR detection as found in the bibliography.

Sensor	Matrix	Method	Linear Range (μM)	LOD (μM)	Ref
ZnNC-ERGO	Water	DPV	0.50–70	0.077	[76]
GCE/NGr	Tablet	AMP	0.10–100	3.030	[77]
GCE/3DCN-NF	Tablet	DPV	0.50–2	0.030	[78]
GCE/Poly(Thr)/GO/MWCNT	Tablet Serum	DPV	5–200	0.160	[79]
SPCE/AgNPs/MWCNT	Tablet Water	SWV	0.50–400	0.240	[80]
CPE/MMT_{k10}	Tablet	DPV	1–15	0.460	[81]
CPE/ERGO/AgNPs	Tablet	CV	0.10–10	0.015	[82]
GCE/gCN-AgPVP	Tablet	SWV	0.20–100	0.079	[83]
GCE/S@ERGO	Tablet	DPV	0.05–125	0.070	[84]
GCE/CuO/O-MWCNT	Tablet	LSV	0.060–1450	0.007	[59]
GCE/ph/ERGO	Tablet	SWV	0.10–0.80	0.018	This work

ZnNC: Zn/N-doped carbon; DPV: Differential pulse voltammetry; NGr: Nitrogen-doped graphene; AMP: Amperometry; 3DCN-NF: 3D carbon nanoporous dispersed in Nafion; Poly(Thr): poly-l-threonine; GO: Graphene oxide; MWCNT: Multi-walled carbon nanotube; SPCE: Screen-printed carbon electrode; AgNPs: Silver nanoparticles; CPE: Carbon paste electrode; MMT_{k10}: potassium montmorillonite clay; gCN-AgPVP: graphitic carbon nitride-silver polyvinylpyrrolidone; S@ERGO: sulfur-doped reduced graphene oxide; CuO: Cupric oxide; O-MWCNT: Opened multiwalled carbon nanotube; LSV: Linear sweep voltammetry.

2.7.2. Repeatability and Reproducibility Studies

The repeatability of the proposed GCE/ph/ERGO electrode was assessed through the stability of a 0.30 μM PAR current signal in a series of 14 measurements with one electrode under optimized conditions. Figure 4C shows a constant peak current with a relative standard deviation (RSD) of 2.22%, which indicates good precision. To evaluate the sensor reproducibility, four different electrodes were prepared and used to determine the current of 0.30 μM PAR under optimized conditions (Figure 4D), resulting in a 7.64% RDS value. In addition, the stability of the sensor was tested by measuring the response 24 h after its modification, and no significant signal loss was found, validating the consistency and robustness of the fabricated sensor.

2.7.3. Excipient Analysis

The influence of various excipients commonly used in PAR pharmaceutical formulations was assessed to evaluate the systematic applicability of the proposed electrochemical sensor. The excipient analysis was conducted using the SWV method under optimized conditions for the fabricated electrode, incorporating a 10- and 100-fold excess of excipients. This study aimed to determine the impact of 1 μM and 10 μM of talc, starch, stearic acid, magnesium stearate, silicon dioxide, and microcrystalline cellulose PH 101 excipients on the peak current of a 0.10 μM PAR signal. Figure S6 shows that only magnesium stearate and microcrystalline cellulose PH 101 cause interference in the 10-fold excess addition and that stearic acid, magnesium stearate, and microcrystalline cellulose PH 101 cause interference in the 100-fold excess addition.

2.8. Accuracy and Application in Real Samples

The accuracy of the proposed methodology was evaluated using a generic pharmaceutical formulation of PAR (paracetamol 500 mg). The pharmaceutical dosage solution was prepared by dissolving a known amount of tablet powder in 100 mL of ethanol. Then, the tablet solution was diluted with 0.10 M acid/acetate buffer pH 5 to prepare the desired concentration of the pharmaceutical sample. The prepared tablet solution analysis was performed using SWV measurements by adding known concentrations of PAR standard to the real pharmaceutical sample by the standard addition method (Figure 5). The results

obtained are in accordance with the labeled content on the tablet, obtaining a recovery percentage of 105% (see Table 2), a slight deviation attributed to minor matrix-induced signal enhancement or analytical variability, which falls well within the AOAC's accepted range for analytical accuracy. These results were compared with HPLC analysis made for the same tablet powder of PAR pharmaceutical dosage by the standard addition method, obtaining a 98% recovery percentage. Therefore, based on the results obtained, we can conclude that the fabricated sensor has a similar performance to the certified HPLC analysis and verifies the effective reliability and validity of the sensor for feasible screening analysis in the pharmaceutical industry.

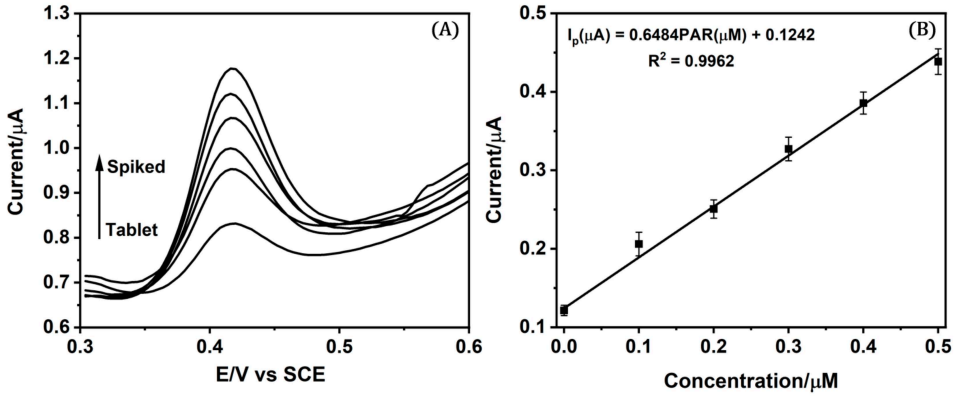

Figure 5. (**A**) Voltammograms and (**B**) calibration plot for the standard addition method applied to pharmaceutical formulations.

Table 2. Recovery percentage obtained from pharmaceutical real sample analysis (n = 3).

Method	Labeled Amount (mM)	Found Amount (mM)	Recovery (%)
GCE/ph/ERGO electrode	5896.18	6212.23	105
HPLC analysis	5896.18	5765.70	98

3. Materials and Methods

3.1. Chemicals and Materials

All reagents are of analytical grade. Ultra-Highly Concentrated Single-Layer Graphene Oxide ($C_xO_yH_z$, 6.2 gL^{-1}) was purchased from Graphene Supermarket (Calverton, NY, USA). Acetaminophen (PAR, $CH_3CONHC_6H_4OH$, 98%), 4-nitroaniline (pNA, $O_2NC_6H_4NH_2$, 99%), sodium nitrite ($NaNO_2$, 97%), potassium chloride (KCl, 99%), potassium ferrocyanide ($K_4[Fe(CN)_6]$, 98.5%) and ferricyanide ($K_3[Fe(CN)_6]$, 99%), disodium hydrogen phosphate (Na_2HPO_4, 99%), sodium dihydrogen phosphate dihydrate ($NaH_2PO_4{\cdot}2H_2O$, 99%), sodium hydroxide (NaOH, 97%), sodium acetate (CH_3COONa, 99%), ammonium chloride (NH_4Cl, 99.5%), boric acid (H_3BO_3, 99.5%), acetic acid (CH_3CO_2H, 99.99%), fuming hydrochloric acid (HCl 37%), phosphoric acid (H_3PO_4, 85%), nitric acid (HNO_3, 65%), sulfuric acid (H_2SO_4, 95–97%), ammonia (NH_3, 99.98%), acetonitrile (CH_3CN, 99.9%), and absolute ethanol (EtOH, CH_3CH_2OH, 99.5%) were purchased from Sigma-Aldrich (Darmstadt, Germany). The acetic/acetate (HAc/Ac^-) buffer solution used in this work contained 0.10 M CH_3COONa and 0.10 M CH_3CO_2H, adjusted to pH 5 with NaOH, and the phosphate buffer solution (PBS) contained 0.10 M Na_2HPO_4, 0.10 M NaH_2PO_4, and 0.10 M H_3PO_4, adjusted to pH 7 with NaOH. The ferro/ferricyanide solution was prepared using 5 mM $K_4Fe(CN)_6$, 5 mM $K_3Fe(CN)_6$, 0.50 M KCl, and PBS. Water miliQ (Burlington, MA, USA) (>18.30 MΩ· cm) was used for the preparation of all

solutions and material cleaning. All the measurements were conducted in an extra pure nitrogen (N_2, 99.995%) atmosphere at ambient temperature (23–26 °C).

3.2. Instrumentation

All electrochemical measurements were performed with a 621E model potentiostat from CH Instruments Inc. (Austin, TX, USA) in an electrochemical cell using a three-electrode system: a glassy carbon working electrode (GCE, CHI104, 3 mm diameter) or GCE/ph/ERGO, saturated calomel reference electrode (SCE), and auxiliary platinum wire electrode. Electrochemical impedance spectroscopy (EIS) measurements were performed in a frequency range from 0.1 to 100,000 Hz with an amplitude of 5 mV. The prepared electrodes were characterized by scanning electron microscopy (SEM) using FE-SEM with a FEI Quanta FEG 250 model from ThermoFisher Scientific (Waltham, MA, USA).

3.3. Fabrication of Sensing Interfaces for Detection

Before use, GCE was polished with a slurry of 0.05 μm alumina powder and then rinsed abundantly with water and dried at room temperature to achieve a clean surface. The preparation of the p-aminophenyl-modified GCE (GCE/pNH_2) used is reported in the literature [29]. A total of 1 mmol L^{-1} $NaNO_2$ was added to a cooled solution of 1 mmol L^{-1} of *p*-nitroaniline (pNA) in 0.50 M aqueous HCl and left in an ice bath for 10 min to generate the nitrophenyl diazonium salt. Then, the electrografting process was conducted in this solution by cyclic voltammetry (CV) from 0.50 to −0.50 V at 100 mV s^{-1} for 2 cycles. The electrode was rinsed with water, acetonitrile, and water. The nitro groups in the modified surface were reduced to amino groups in 1 M KCl ethanolic solution (90%H_2O/10%EtOH) using CV from −0.40 to −1.50 V at 50 mV s^{-1} for 3 cycles. The electrode was rinsed with water, and an aliquot of 5 μL of a solution of 0.50 M HCl, 5 mM $NaNO_2$, and 0.62 g L^{-1} graphene oxide (GO) was deposited on the GCE/pNH_2 electrode surface and allowed to dry at room temperature to convert the external amino group -NH_2 to -N_2 by diazotization, which was displaced by GO due to instability to obtain GCE/ph/GO. The reduction of GO to electrochemically reduced graphene oxide (ERGO) was performed by CV from 0.00 to −1.60 V at 100 mV s^{-1} for 7 cycles in 0.50 M NaCl solution to obtain GCE/ph/ERGO.

3.4. Electrochemistry Measurement of PAR

Square wave voltammetric measurements (SWVs) were performed with a scanning potential from 0.3 to 0.70 V using a step potential of 4 mV, pulse amplitudes of 25 mV, and a frequency of 15 Hz. All measurements were conducted with oxygen removal. Repeated blank measurements were recorded in 10 mL of HAc/Ac^- buffer until a stable background current was obtained. Individual calibrations of PA were performed in 0.10 M HAc/Ac^- buffer at pH 5 by adding increasing concentrations of the analyte in triplicate.

3.5. Sample Preparation

The real sample analysis was performed by SWV and high-performance liquid chromatography (HPLC). PAR commercial tablets were purchased from a local pharmaceutical store, each containing 500 mg of PAR. The tablets were weighed and finely powdered in a mortar and pestle. For HPLC analysis, to the corresponding weight, 25 mL of methanol LiChrosolv® grade was added to obtain a 33.08 mM PAR sample solution, which was shaken and filtered through a 0.45 μm syringe membrane filter, and an appropriate volume of the PAR solution was diluted to 50 mL with a 10 mM PBS pH 7.5 buffer and methanol mixture. The measurement conditions were 1 mL min^{-1} flow rate, 10 μL injection volume, 8 min run time, 220 nm UV/vis detector, and 80 PBS/20 methanol mobile phase. For SWV measurements, a known amount of PAR tablet powder was dissolved in 100 mL of ethanol, and then the tablet solution was diluted with 0.10 M acid/acetate buffer pH 5 to obtain a

0.10 mM PAR sample solution. The prepared tablet solution analysis was performed using SWV measurements by adding known concentrations of the prepared PAR standard to the real pharmaceutical sample by the standard addition method.

4. Conclusions

The study describes the fabrication and characterization of an electrochemically reduced graphene oxide immobilized in a glassy carbon electrode sensor with electrografting of phenyl diazonium salts. The combination was chosen to improve the sensor surface stability, conductivity, and sensitivity toward phenolic compounds like paracetamol. The resulting robust and sensitive surface showed an obvious increase in the PAR detection signal compared to unmodified electrodes or only ERGO electrodes. Under optimized conditions, PAR was detected in the presence of interfering excipients in 10- and 100-fold excess, with good RSD results in repeatability and reproducibility tests. The linear range and LOD obtained are comparable with those found in the literature for PAR detection with voltammetric techniques. The new sensing platform proved to be sensitive in pharmaceutical matrices, with recovery close to 100%, comparable with accepted techniques such as HPLC. Although this work focused on PAR detection due to its pharmaceutical relevance and redox activity, the electrode modification could be extended to other electroactive drugs with similar structures, such as catecholamines or other phenolic pharmaceuticals, such as Ibuprofen, Caffeine, and Rutin, among others. Finally, while the sensor demonstrates excellent sensitivity toward paracetamol in pharmaceutical formulations, and its design is intended for analytical detection rather than pollutant removal or membrane-based purification, it could be potentially used to detect PAR as an emergent contaminant in aqueous samples, provided that an analysis of possible interferents present in wastewater is made.

Supplementary Materials: The following supporting information can be downloaded at: https://www.mdpi.com/article/10.3390/ijms26094267/s1.

Author Contributions: Conceptualization, A.P.d.l.v.; methodology, A.P.d.l.v.; investigation, A.P.d.l.v.; writing—original draft preparation, A.P.d.l.v.; writing—review and editing, A.P.d.l.v., F.L., B.P., J.P., R.S. and M.J.A.; supervision, R.S. and M.J.A.; funding acquisition, A.P.d.l.v. and R.S. All authors have read and agreed to the published version of the manuscript.

Funding: This research was funded by The Santiago of Chile University's Directorate of Scientific and Technological Research (Dicyt-USACH) 022142 SS_Postdoc/USA1956 (R. Segura), the National Fund for Scientific and Technological Development (FONDECYT) 1230628 (R. Segura), the fund for Scholarship Support for Research Thesis and Student Mobility of the Faculty of Chemistry and Biology (FyQ, USACH) years 2020 to 2024.

Institutional Review Board Statement: Not applicable.

Informed Consent Statement: Not applicable.

Data Availability Statement: The raw data supporting the conclusions of this article will be made available by the authors upon request.

Acknowledgments: The authors acknowledge the National Agency for Research and Development (ANID) through the Millennium Institute on Green Ammonia as Energy Vector (MIGA) Science Initiative Program/ICN2021_023, Scientific and Technological Equipment Program (FONDEQUIP) EQM 190016, and FONDEQUIP EQM160036.

Conflicts of Interest: The authors declare no conflicts of interest.

References

1. World Health Organization (WHO). WHO Certification Scheme on the Quality of Pharmaceutical Products Moving in International Commerce: Proposed Guidelines for the Certification of Active Pharmaceutical Ingredients. 1997. Available online: https://apps.who.int/iris/handle/10665/63628 (accessed on 10 February 2025).
2. Athersuch, T.J.; Antoine, D.J.; Boobis, A.R.; Coen, M.; Daly, A.K.; Possamai, L.; Nicholson, K.; Wilson, I.D. Paracetamol metabolism; hepatotoxicity, biomarkers and therapeutic interventions: A perspective. *Toxicol. Res.* **2018**, *7*, 347–357. [CrossRef] [PubMed]
3. Jasani, B.; Weisz, D.E.; Mcnamara, P.J. Evidence-based use of acetaminophen for hemodynamically significant ductus arteriosus in preterm infants. *Semin. Perinatol.* **2018**, *42*, 243–252. [CrossRef]
4. Rajaram, P.; Subramanian, R. Management of Acute Liver Failure in the Intensive Care Unit Setting. *Clin. Liver Dis.* **2018**, *22*, 403–408. [CrossRef]
5. Mcgill, M.R.; Jaeschke, H. Expert Review of Molecular Diagnostics Biomarkers of drug-induced liver injury: Progress and utility in research, medicine, and regulation. *Expert Rev. Mol. Diagn.* **2018**, *18*, 797–807. [CrossRef] [PubMed]
6. World Health Organization (WHO). WHO Guidance on Testing of "Suspect" Falsified Medicines—TRS 1010—Annex 5. 2018. Available online: https://www.who.int/publications/m/item/trs1010-annex5 (accessed on 10 February 2025).
7. World Health Organization (WHO). WHO Good Practices for Pharmaceutical Quality Control Laboratories—TRS 957—Annex 1. 2010. Available online: https://www.who.int/publications/m/item/trs957-annex1 (accessed on 12 February 2025).
8. World Health Organization (WHO). *WHO Considerations for Requesting Analysis of Medicines Samples—TRS 1010—Annex 3*; WHO Technical Report Series 1010; Annex: Manassas, VA, USA, 2018; Volume 3, pp. 179–186. Available online: https://www.who.int/publications/m/item/trs1010-annex3 (accessed on 12 February 2025).
9. Kim, C.; Ryu, H.D.; Chung, E.G.; Kim, Y.; Lee, J.K. A review of analytical procedures for the simultaneous determination of medically important veterinary antibiotics in environmental water: Sample preparation, liquid chromatography, and mass spectrometry. *J. Environ. Manag.* **2018**, *217*, 629–645. [CrossRef] [PubMed]
10. Mishra, S.; Singh, S.P.; Kumar, P.; Khan, M.A.; Singh, S. Emerging electrochemical portable methodologies on carbon-based electrocatalyst for the determination of pharmaceutical and pest control pollutants: State of the art. *J. Environ. Chem. Eng.* **2023**, *11*, 109023. [CrossRef]
11. Satish, S.; Dey, A.; Tharmavaram, M.; Khatri, N.; Rawtani, D. Risk assessment of selected pharmaceuticals on wildlife with nanomaterials based aptasensors. *Sci. Total Environ.* **2022**, *836*, 155622. [CrossRef]
12. Kurbanoglu, S.; Ozkan, S.A. Electrochemical carbon based nanosensors: A promising tool in pharmaceutical and biomedical analysis. *J. Pharm. Biomed. Anal.* **2018**, *147*, 439–457. [CrossRef]
13. Megale, J.D.; De Souza, D. New approaches in antibiotics detection: The use of square wave voltammetry. *J. Pharm. Biomed. Anal.* **2023**, *234*, 115526. [CrossRef]
14. Montaseri, H.; Forbes, P.B.C. Analytical techniques for the determination of acetaminophen: A review. *TrAC—Trends Anal. Chem.* **2018**, *108*, 122–134. [CrossRef]
15. Gorski, W.; Electrodes, C.M.; Alkire, R.C.; Lipkowski, J.; Kolb, D.M.; Ross, P.N. (Eds.) *Advances in Electrochemical Science and Engineering*; Wiley-VCH John Wiley & Sons: Weinheim, Germany, 2010; p. 6274. [CrossRef]
16. Boumya, W.; Taoufik, N.; Achak, M.; Barka, N. Chemically modified carbon-based electrodes for the determination of paracetamol in drugs and biological samples. *J. Pharm. Anal.* **2021**, *11*, 138–154. [CrossRef]
17. Lakhera, P.; Chaudhary, V.; Jha, A.; Singh, R.; Kush, P.; Kumar, P. Recent developments and fabrication of the different electrochemical biosensors based on modified screen printed and glassy carbon electrodes for the early diagnosis of diverse breast cancer biomarkers. *Mater. Today Chem.* **2022**, *26*, 101129. [CrossRef]
18. Ren, S.; Zeng, J.; Zheng, Z.; Shi, H. Perspective and application of modified electrode material technology in electrochemical voltammetric sensors for analysis and detection of illicit drugs. *Sens. Actuators A Phys.* **2021**, *329*, 112821. [CrossRef]
19. Baig, N.; Sajid, M.; Saleh, T.A. Recent trends in nanomaterial-modified electrodes for electroanalytical applications. *TrAC—Trends Anal. Chem.* **2019**, *111*, 47–61. [CrossRef]
20. Wang, D.; Khan, M.K.; Moloney, M.G. Diazo and diazonium compounds for surface modification. *Tetrahedron Lett.* **2020**, *61*, 151672. [CrossRef]
21. Pilan, L. Tailoring the performance of electrochemical biosensors based on carbon nanomaterials via aryldiazonium electrografting. *Bioelectrochemistry* **2021**, *138*, 107697. [CrossRef]
22. Pinson, J.; Podvorica, F.I. Surface modification of materials: Electrografting of organic films. *Curr. Opin. Electrochem.* **2020**, *24*, 44–48. [CrossRef]
23. Morales-Martínez, D.; González, F.J. A mechanistic approach to the electrografting of carbon surfaces and electrochemical properties of the grafted films—A critical review. *Electrochim. Acta* **2022**, *425*, 140693. [CrossRef]
24. Patra, S.; Roy, E.; Tiwari, A.; Madhuri, R.; Sharma, P.K. 2-Dimensional graphene as a route for emergence of additional dimension nanomaterials. *Biosens. Bioelectron.* **2017**, *89*, 8–27. [CrossRef]
25. Kochmann, S. *Graphene as a Sensor Material*; Universitat Regensburg: Regensburg, Germany, 2013.

26. Zhou, A.; Bai, J.; Hong, W.; Bai, H. Electrochemically reduced graphene oxide: Preparation, composites, and applications. *Carbon* **2022**, *191*, 301–332. [CrossRef]
27. Zhang, H.; He, R.; Niu, Y.; Han, F.; Li, J.; Zhang, X.; Xu, F. Graphene-enabled wearable sensors for healthcare monitoring. *Biosens. Bioelectron.* **2022**, *197*, 113777. [CrossRef] [PubMed]
28. Badillo-Ramírez, I.; Carreón, Y.J.P.; Rodríguez-Almazán, C.; Medina-Durán, C.M.; Islas, S.R.; Saniger, J.M. Graphene-Based Biosensors for Molecular Chronic Inflammatory Disease Biomarker Detection. *Biosensors* **2022**, *12*, 244. [CrossRef] [PubMed]
29. Ni, S.; Qiao, L.; Shen, Z.; Gao, Y.; Liu, G. Physical absorption vs. covalent binding of graphene oxide on glassy carbon electrode towards a robust aptasensor for ratiometric electrochemical detection of vascular endothelial growth factor (VEGF) in serum. *Electrochim. Acta* **2020**, *331*, 135321. [CrossRef]
30. Hetemi, D.; Noël, V.; Pinson, J. Grafting of diazonium salts on surfaces: Application to biosensors. *Biosensors* **2020**, *10*, 4. [CrossRef]
31. Candia, C.P.; Imbarack, E.; Silva, C.P.; Olguín, C.F.; Jara, G.; Fuentes, S.; Zagal, J.H.; Agurto, N.; Pavez, J. Covalent modification of glassy carbon surface via radical-induced grafting from electrochemical oxidation of imine derivatives. *Electrochim. Acta* **2023**, *459*, 142544. [CrossRef]
32. Li, D.; Luo, Y.; Onidas, D.; He, L.; Jin, M.; Gazeau, F.; Pinson, J.; Mangeney, C. Surface functionalization of nanomaterials by aryl diazonium salts for biomedical sciences. *Adv. Colloid. Interface Sci.* **2021**, *294*, 102479. [CrossRef]
33. Mohamed, A.A.; Salmi, Z.; Dahoumane, S.A.; Mekki, A.; Carbonnier, B.; Chehimi, M.M. Functionalization of nanomaterials with aryldiazonium salts. *Adv. Colloid. Interface Sci.* **2015**, *225*, 16–36. [CrossRef]
34. Borane, N.; Boddula, R.; Odedara, N.; Singh, J.; Andhe, M.; Patel, R. Comprehensive review on synthetic methods and functionalization of graphene oxide: Emerging Applications. *Nano-Struct. Nano-Objects* **2024**, *39*, 101282. [CrossRef]
35. Gautier, C.; López, I.; Breton, T. A post-functionalization toolbox for diazonium (electro)-grafted surfaces: Review of the coupling methods. *Mater. Adv.* **2021**, *2*, 2773–2810. [CrossRef]
36. Alam, M.A. Graphene based electrochemical biosensors for the detection of cardiac biomarkers. *Biosens. Bioelectron. X* **2024**, *20*, 100515. [CrossRef]
37. Devi, K.S.S.; Prakash, J.; Tsujimura, S. Graphene oxide-based nanomaterials for electrochemical bio/immune sensing and its advancements in health care applications: A review. *Hybrid. Adv.* **2024**, *5*, 100123. [CrossRef]
38. Bouden, S.; Pinson, J.; Vautrin-Ul, C. Electrografting of diazonium salts: A kinetics study. *Electrochem. Commun.* **2017**, *81*, 120–123. [CrossRef]
39. Huynh, T.M.T.; Tahara, K.; De Feyter, S.; Phan, T.H. On the role of functional groups in the formation of diazonium based covalent attachments: Dendritic vs. layer-by-layer growth. *RSC Adv.* **2023**, *13*, 24576–24582. [CrossRef]
40. Cao, C.; Jin, R.; Wei, H.; Yang, W.; Goldys, E.M.; Hutchinson, M.R.; Liu, S.; Chen, X.; Yang, G.; Liu, G. Graphene Oxide Based Recyclable in Vivo Device for Amperometric Monitoring of Interferon-γ in Inflammatory Mice. *ACS Appl. Mater. Interfaces* **2018**, *10*, 33078–33087. [CrossRef]
41. Shul, G.; Ruiz, C.A.C.; Rochefort, D.; Brooksby, P.A.; Bélanger, D. Electrochemical functionalization of glassy carbon electrode by reduction of diazonium cations in protic ionic liquid. *Electrochim. Acta* **2013**, *106*, 378–385. [CrossRef]
42. Wu, T.; Fitchett, C.M.; Brooksby, P.A.; Downard, A.J. Building Tailored Interfaces through Covalent Coupling Reactions at Layers Grafted from Aryldiazonium Salts. *ACS Appl. Mater. Interfaces* **2021**, *13*, 11545–11570. [CrossRef]
43. Wu, T.; Fitchett, C.M.; Downard, A.J. Para-Fluoro-Thiol Reaction on Anchor Layers Grafted from an Aryldiazonium Salt: A Tool for Surface Functionalization with Thiols. *Langmuir* **2021**, *37*, 11397–11405. [CrossRef] [PubMed]
44. Liendo, F.; de la Vega, A.P.; Jesus Aguirre, M.; Godoy, F.; Martí, A.A.; Flores, E.; Pizarro, J.; Segura, R. A simple graphene modified electrode for the determination of antimony(III) in edible plants and beverage. *Food Chem.* **2022**, *367*, 130676. [CrossRef]
45. Bui-Thi-Tuyet, V.; Cannizzo, C.; Legros, C.; Andrieux, M.; Chaussé, A. Modification of fluorine-doped tin oxide surface: Optimization of the electrochemical grafting of diazonium salt. *Surf. Interfaces* **2019**, *15*, 110–116. [CrossRef]
46. Rather, J.A.; Khudaish, E.A.; Munam, A.; Qurashi, A.; Kannan, P. Electrochemically reduced fullerene–graphene oxide interface for swift detection of Parkinsons disease biomarkers. *Sens. Actuators B Chem.* **2016**, *237*, 672–684. [CrossRef]
47. Kesavan, S.; Kumar, D.R.; Baynosa, M.L.; Shim, J.J. Potentiodynamic formation of diaminobenzene films on an electrochemically reduced graphene oxide surface: Determination of nitrite in water samples. *Mater. Sci. Eng. C* **2018**, *85*, 97–106. [CrossRef]
48. Khudaish, E.A.; Myint, M.T.Z.; Rather, J.A. A solid-state sensor based on poly(2,4,6-triaminopyrimidine) grafted with electrochemically reduced graphene oxide: Fabrication, characterization, kinetics and potential analysis on ephedrine. *Microchem. J.* **2019**, *147*, 444–453. [CrossRef]
49. Kesavan, S.; Gowthaman, N.S.K.; Alwarappan, S.; John, S.A. Real time detection of adenosine and theophylline in urine and blood samples using graphene modified electrode. *Sens. Actuators B Chem.* **2019**, *278*, 46–54. [CrossRef]
50. Park, S.; Ruoff, R.S. Chemical methods for the production of graphenes. *Nat. Nanotechnol.* **2009**, *4*, 217–224. [CrossRef] [PubMed]
51. Saby, C.; Ortiz, B.; Champagne, G.Y.; Bélanger, D. Electrochemical Modification of Glassy Carbon Electrode Using Aromatic Diazonium Salts. 1. Blocking Effect of 4-Nitrophenyl and 4-Carboxyphenyl Groups. *Langmuir* **1997**, *13*, 6805–6813. [CrossRef]

52. Pinson, J.; Podvorica, F. Attachment of organic layers to conductive or semiconductive surfaces by reduction of diazonium salts. *Chem. Soc. Rev.* **2005**, *34*, 429. [CrossRef] [PubMed]
53. Menanteau, T.; Dabos-Seignon, S.; Levillain, E.; Breton, T. Impact of the Diazonium Grafting Control on the Interfacial Reactivity: Monolayer versus Multilayer. *Chem. Electro. Chem.* **2017**, *4*, 278–282. [CrossRef]
54. Tehrani, Z.; Abbasi, H.Y.; Devadoss, A.; Evans, J.E.; Guy, O.J. Assessing Surface Coverage of Aminophenyl Bonding Sites on Diazotised Glassy Carbon Electrodes for Optimised Electrochemical Biosensor Performance. *Nanomaterials* **2021**, *11*, 416. [CrossRef]
55. Liendo, F.; Pichún, B.; de la Vega, A.P.; Penagos, J.; Serrano, N.; Díaz-Cruz, J.M.; Pizarro, J.; Segura, R.; Aguirre, M.J. Electrochemical Sensor Based on Glassy Carbon Electrode Modified with Carbon Nanohorns (SWCNH) for Determination of Cr(VI) via Adsorptive Cathodic Stripping Voltammetry (AdCSV) in Tap Water. *Nanomaterials* **2024**, *14*, 1465. [CrossRef]
56. Arancibia, V.; Penagos-Llanos, J.; Nagles, E.; García-Beltrán, O.; Hurtado, J.J. Development of a microcomposite with single-walled carbon nanotubes and Nd_2O_3 for determination of paracetamol in pharmaceutical dosage by adsorptive voltammetry. *J. Pharm. Anal.* **2019**, *9*, 62–69. [CrossRef]
57. Ashoka, N.B.; Swamy, B.E.K.; Jayadevappa, H.; Sharma, S.C. Simultaneous electroanalysis of dopamine, paracetamol and folic acid using TiO_2-WO_3 nanoparticle modified carbon paste electrode. *J. Electroanal. Chem.* **2020**, *859*, 113819. [CrossRef]
58. Changsan, N.; Chairam, S.; Jarujamrus, P.; Amatatongchai, M. Sensitive electrochemical sensor based on gold nanoparticles assembled ferrocene-functionalised graphene oxide modified glassy carbon electrode for simultaneous determination of dopamine and acetaminophen. *Adv. Nat. Sci. Nanosci. Nanotechnol.* **2022**, *13*, 015012. [CrossRef]
59. Richard, Y.A.; Lincy, S.A.; Lo, A.-Y.; Koventhan, C.; Dharuman, V.; Piraman, S. Electrochemical investigation of an antipyretic drug in plant extracts and environmental samples at the O-MWCNT/CuO nanostructure modified glassy carbon electrode. *Environ. Sci. Nano* **2025**, *12*, 909–923. [CrossRef]
60. Gharous, M.; Bounab, L.; Pereira, F.J.; Choukairi, M.; López, R.; Aller, A.J. Electrochemical Kinetics and Detection of Paracetamol by Stevensite-Modified Carbon Paste Electrode in Biological Fluids and Pharmaceutical Formulations. *Int. J. Mol. Sci.* **2023**, *24*, 11269. [CrossRef]
61. Stoytcheva, M.; Velkova, Z.; Gochev, V.; Valdez, B.; Curiel, M. Advances in electrochemical sensors for paracetamol detection: Electrode materials, modifications, and analytical applications. *Int. J. Electrochem. Sci.* **2025**, *20*, 100924. [CrossRef]
62. Phong, N.H.; Toan, T.T.T.; Tinh, M.X.; Tuyen, T.N.; Mau, T.X.; Khieu, D.Q. Simultaneous Voltammetric Determination of Ascorbic Acid, Paracetamol, and Caffeine Using Electrochemically Reduced Graphene-Oxide-Modified Electrode. *J. Nanomater.* **2018**, *2018*, 5348016. [CrossRef]
63. Serrano, N.; Castilla, Ò.; Ariño, C.; Diaz-Cruz, M.S.; Díaz-Cruz, J.M. Commercial screen-printed electrodes based on carbon nanomaterials for a fast and cost-effective voltammetric determination of paracetamol, ibuprofen and caffeine in water samples. *Sensors* **2019**, *19*, 4039. [CrossRef]
64. Sousa Pereira, A.C.; Nunes da Silva, D.; Sales Porto, L.; César Pereira, A. Development of Electrochemical Biosensor Based on Nanostructured Carbon Materials for Paracetamol Determination. *Electroanalysis* **2020**, *32*, 1905–1913. [CrossRef]
65. Nematollahi, D.; Shayani-Jam, H.; Alimoradi, M.; Niroomand, S. Electrochemical oxidation of acetaminophen in aqueous solutions: Kinetic evaluation of hydrolysis, hydroxylation and dimerization processes. *Electrochim. Acta* **2009**, *54*, 7407–7415. [CrossRef]
66. Geczo, A.; Giannakoudakis, D.A.; Triantafyllidis, K.; Elshaer, M.R.; Rodríguez-Aguado, E.; Bashkova, S. Mechanistic insights into acetaminophen removal on cashew nut shell biomass-derived activated carbons. *Environ. Sci. Pollut. Res.* **2021**, *28*, 58969–58982. [CrossRef]
67. Narouie, S.; Rounaghi, G.H.; Saravani, H.; Shahbakhsh, M. Iodine/iodide-doped polymeric nanospheres for simultaneous voltammetric detection of p-aminophenol, phenol, and p-nitrophenol. *Microchim. Acta* **2022**, *189*, 267. [CrossRef]
68. Clares, P.; Pérez-Ràfols, C.; Serrano, N.; Díaz-Cruz, J.M. Voltammetric Determination of Active Pharmaceutical Ingredients Using Screen-Printed Electrodes. *Chemosensors* **2022**, *10*, 95. [CrossRef]
69. Ninham, B.W.; Parsegian, V.A. Electrostatic potential between surfaces bearing ionizable groups in ionic equilibrium with physiologic saline solution. *J. Theor. Biol.* **1971**, *31*, 405–428. [CrossRef] [PubMed]
70. Cabezas, A.; Aguilera, S.; Urzúa, S.A.; Cooper, C.D.; Vera, C.; Aguirre, M.; Márquez, P.; Pizarro, J. Hematite nanoparticle-modified carbon paper as a promising electrochemical sensor for atropine detection in beverages. *Food Chem.* **2025**, *474*, 143187. [CrossRef]
71. Pizarro, J.; Segura, R.; Tapia, D.; Bollo, S.; Sierra-Rosales, P. Electroanalytical Determination of Cd(II) and Pb(II) in Bivalve Mollusks using Electrochemically Reduced Graphene Oxide-based Electrode. *Electroanalysis* **2019**, *31*, 2199–2205. [CrossRef]
72. Segura, R.; Pizarro, J.; Díaz, K.; Placencio, A.; Godoy, F.; Pino, E.; Recio, F. Development of electrochemical sensors for the determination of selenium using gold nanoparticles modified electrodes. *Sens. Actuators B Chem.* **2015**, *220*, 263–269. [CrossRef]
73. Pichún, B.; Núñez, C.; Arancibia, V.; Martí, A.A.; Aguirre, M.J.; Pizarro, J.; Segura, R.; Flores, E. Enhanced voltammetric sensing platform based on gold nanorods and electrochemically reduced graphene oxide for As(III) determination in seafood samples. *J. Appl. Electrochem.* **2023**, *54*, 1595–1606. [CrossRef]

74. Navarro, F.; Segura, R.; Godoy, F.; Martí, A.A.; Mascayano, C.; Aguirre, M.J.; Flores, E.; Pizarro, J. Fast and Simple Preparation of a Sensor Based on Electrochemically Reduced Graphene Oxide (rGO) for the Determination of Zopiclone in Pharmaceutical Dosage by Square Wave Adsorptive Stripping Voltammetry (SWAdSV). *Electroanalysis* **2023**, *35*, e202200357. [CrossRef]
75. Penagos-Llanos, J.; Segura, R.; de la Vega, A.P.; Pichun, B.; Liendo, F.; Riesco, F.; Nagles, E. Electrochemical Determination of Uric Acid Using a Nanocomposite Electrode with Molybdenum Disulfide/Multiwalled Carbon Nanotubes (MoS2@MWCNT). *Nanomaterials* **2024**, *14*, 958. [CrossRef]
76. Shih, Y.-J.; Wu, Z.-L.; Lin, S.-K. Electrochemical detection of paracetamol using zeolitic imidazolate framework and graphene oxide derived zinc/nitrogen-doped carbon. *Sens. Actuators B Chem.* **2024**, *409*, 135600. [CrossRef]
77. Magerusan, L.; Pogacean, F.; Pruneanu, S. Enhanced Acetaminophen Electrochemical Sensing Based on Nitrogen-Doped Graphene. *Int. J. Mol. Sci.* **2022**, *23*, 14866. [CrossRef]
78. Cabas Rodriguez, J.A.; Bonetto, A.; Alaniz, R.D.; Zón, M.A.; Pierini, G.D.; Coneo Rodriguez, R.; Planes, G.; Fernández, H.; Arévalo, F.J.; Granero, A.M. Electrochemical sensor based on a glassy carbon electrode modified with a 3D carbon nanoporous composite for the detection of paracetamol in pharmaceutical samples. *J. Electroanal. Chem.* **2024**, *973*, 118689. [CrossRef]
79. Venkata Prasad, G.; Vinothkumar, V.; Joo Jang, S.; Eun Oh, D.; Hyun Kim, T. Multi-walled carbon nanotube/graphene oxide/poly(threonine) composite electrode for boosting electrochemical detection of paracetamol in biological samples. *Microchem. J.* **2023**, *184*, 108205. [CrossRef]
80. Weheabby, S.; Wu, Z.; Al-Hamry, A.; Pašti, I.A.; Anurag, A.; Dentel, D.; Tegenkamp, C.; Kanoun, O. Paracetamol detection in environmental and pharmaceutical samples using multi-walled carbon nanotubes decorated with silver nanoparticles. *Microchem. J.* **2023**, *193*, 109192. [CrossRef]
81. Achache, M.; Elouilali Idrissi, G.; Chraka, A.; Ben Seddik, N.; Draoui, K.; Bouchta, D.; Mohamed, C. Detection of paracetamol by a montmorillonite-modified carbon paste sensor: A study combining MC simulation, DFT computation and electrochemical investigations. *Talanta* **2024**, *274*, 126027. [CrossRef] [PubMed]
82. Khelifi, C.; Aitout, R.; Makhloufi, L.; Mahouche-Chergui, S. Eco-friendly synthesis of rGO/AgNPs hybrid nanomaterial for an efficient electrochemical Sensor: Simultaneous detection of paracetamol and caffeine in Pharmaceuticals. *Microchem. J.* **2025**, *212*, 113545. [CrossRef]
83. Mekgoe, N.; Mabuba, N.; Pillay, K. Graphic Carbon Nitride-SilverPolyvinylpyrrolidone Nanocomposite Modified on a Glassy Carbon Electrode for Detection of Paracetamol. *Front. Sens.* **2022**, *3*, 827954. [CrossRef]
84. Khan, M.Q.; Kumar, P.; Khan, R.A.; Ahmad, K.; Kim, H. Fabrication of Sulfur-Doped Reduced Graphene Oxide Modified Glassy Carbon Electrode (S@rGO/GCE) Based Acetaminophen Sensor. *Inorganics* **2022**, *10*, 218. [CrossRef]